I. The Generalized Valence Bond Description of O_2.

II. Configuration Interaction Studies on Low-Lying States of O_2.

Thesis by

BARRY JOEL MOSS

In Partial Fulfillment of the Requirements

For the Degree of

Master of Science

California Institute of Technology

Pasadena, California

1975

(Submitted January 10, 1975)

ABSTRACT

I. The Generalized Valence Bond Description of O_2

Ab initio calculations using the generalized valence bond (GVB) method have been carried out for the lowest triplet and singlet states of O_2 at internuclear distances (R) between $2a_0$ and $6a_0$. In contrast to other orbital descriptions, GVB leads correctly to ground state oxygen atoms as the bond length is increased to infinity. This proper behavior requires optimization of the spatial orbitals themselves and of the permutational coupling between them as well. Analysis of the results as a function of R is straightforward. Constructing a simple configuration interaction (CI) wavefunction using the GVB orbitals leads to excellent potential curves, accounting for 94% of the bond dissociation energy. The calculated adiabatic separation of the singlet and triplet states is 1.09 eV compared with the experimental T_e of 1.01 eV.

II. Configuration Interaction Studies on Low-Lying States of O_2

Configuration interaction calculations are reported as a function of R for the nine state of O_2 corresponding to the $(3\sigma_g)^2 (1\pi_u)^4 (1\pi_g)^2$ and $(3\sigma_g)^2 (1\pi_u)^3 (1\pi_g)^3$ configurations ($X^3\Sigma_g^-$, $a^1\Delta_g$, $b^1\Sigma_g^+$, $^1\Sigma_u^-$, $^3\Delta_u$, $A^3\Sigma_u^+$, $B^3\Sigma_u^-$, $^1\Delta_u$, $^1\Sigma_u^+$). By using the generalized valence bond (GVB) orbitals of the $X^3\Sigma_g^-$ state we obtain good quality GVB-CI wavefunctions with only a moderate number of configurations (72 to 98 spatial configurations) despite the use of a large basis set (double-zeta plus polarization functions). The calculated D_e for the $X^3\Sigma_u^-$ state is 4.88 eV, 93% of the experimental value. The calculated adiabatic excitation energies are on the average about 0.1 eV from the experimental values.

PART ONE:

The Generalized Valence Bond Description of O_2

I.   INTRODUCTION

An early major success for the molecular orbital (MO) description of molecules was obtained for O_2 where Mulliken[4] predicted a triplet ground state and two very low-lying singlet states (1-2 eV), all later verified by experiment.[5] In contrast, a simple valence bond (VB) description $:\overset{..}{O} = \overset{..}{O}:$ suggests a singlet ground state.[6] However, despite the useful description at small internuclear distance (R, the MO wavefunction cannot lead to ground state oxygen atoms as the molecule is pulled apart. Indeed, at large R a simple VB wavefunction would be better.

Since we are interested in studying formation of various states of O_2 from O atoms, neither the MO nor VB methods are suitable. The simplest wavefunction leading to a proper description as O_2 dissociates is the generalized valence bond (GVB) wavefunction.[7-9] The GVB wavefunction is a generalization of the VB wavefunction in which the orbitals are solved for self-consistently (rather than taken as atomic). Alternately, the GVB method can be considered to be a generalization of the MO or Hartree-Fock (HF) method in which dominant pair-correlation effects are included self-consistently.

A special point in this paper is the self-consistent optimization of the permutation coupling of the orbitals (hereafter referred to as orbital coupling). In calculations on large molecules it has generally been convenient to couple various orbital pairs in either a singlet or triplet manner, as this greatly simplifies the variational equations.[10] However, in O_2 we find that the optimum orbital coupling changes markedly as the bond is stretched from the equilibrium bond length (R_e) to infinity and that these changes must be included to permit proper dissociation. In order to allow for this and yet retain computational tractability, a new formulation[11] of the GVB equations has been made to facilitate these studies.

## II. QUALITATIVE GVB DESCRIPTION OF O_2

A. Near R_e

In order to provide a framework for discussing the calculations, we first consider the various ways of orienting the atomic orbitals of two oxygen atoms to form O_2. The ground ^3P state of oxygen atom has the configuration $(1s)^2(2s)^2(2p)^4$. Ignoring the (1s) and (2s) electrons, we can visualize this as

(1)
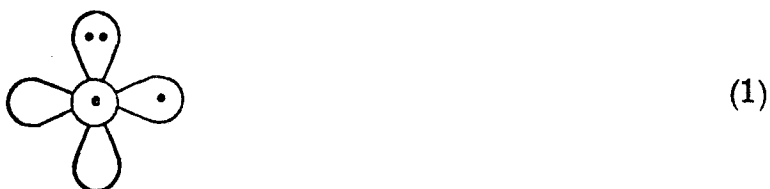
where the two lobed figures such as represent p orbitals in the plane, and represents a p orbital pointing out of the plane. The dots indicate the number of electrons in each orbital.

As there are three possible orientations of (1) (corresponding to the three components of a ^3P state), there are nine ways of pairing two ground state atoms. Including spin, this gives rise to a total of 81 possible (unique) states of O_2. However, we are only interested in those states that can result in a strong bond. Thus, we will consider only those cases in which two singly-occupied orbitals are oriented so that a sigma bond can be formed

(2a)

(2b)

(3a)

(3b)
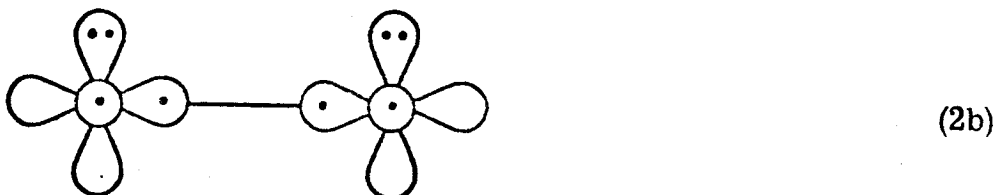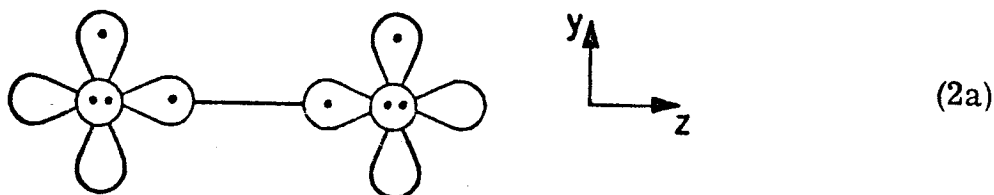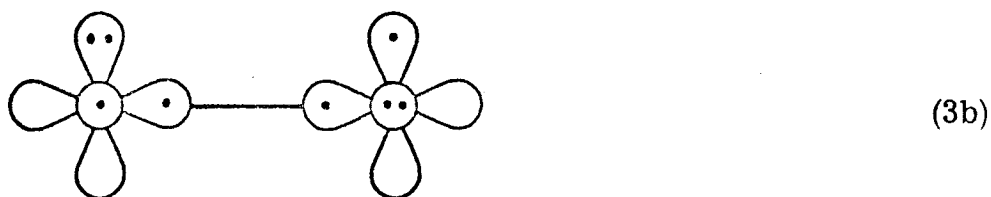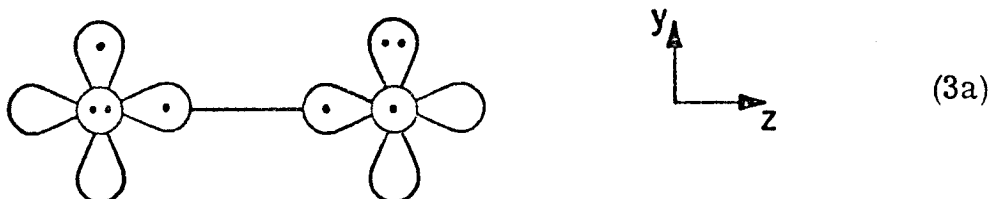
where the straight line connecting the orbitals comprising the sigma bond

indicates that they are   singlet-paired.

Configurations (2a) and (2b) are equivalent and each leads to triplet and

singlet states with the singlet state much lower (a π bond); thus we will consider

only the singlet state in the following.

Configurations (3a) and (3b) are equivalent and each leads to a singlet and

triplet state; in this case the unpaired orbitals $[p_{y\ell}$ and p_{xr} of (3a)$]$ are

orthogonal so that the singlet and triplet states differ only in the exchange

integral

$$E_{3a}^{T} = E_0 - K_{y\ell,xr}$$

$$E_{3a}^{S} = E_0 + K_{y\ell,xr}$$

(4)

and hence the triplet state must be lower.

In order to compare the energies of (2a) and (3a) we must also consider the doubly-occupied π orbitals. In (2a) we form a π bond in the yz plane, but in the xz plane there are doubly-occupied π_x orbitals on each oxygen, leading to large repulsive interactions. On the other hand, in (3a) each doubly-occupied orbital overlaps a singly-occupied orbital. This allows the doubly-occupied orbital to delocalize onto the adjacent center, leading to a significant reduction in the electron repulsion between the electrons in this orbital and in the kinetic energies while maintaining a low nuclear-attraction energy (that is, the doubly-occupied orbital gets bonding character). Because of the Pauli principle, the singly-occupied orbital starting on the second center must get orthogonal to the delocalized doubly-occupied orbital, leading to considerable antibonding character. However the net effect of the doubly-occupied orbital dominates, leading to a net bonding of ~ 30 kcal for each three-electron π bond.[8,12] In contrast, for (2a) each doubly-occupied orbital must get orthogonal to the other (essentially because of the Pauli principle), leading to antibonding rather than bonding interactions.

From these considerations we expect the best configuration of O_2 to be (3) and for the triplet state to be the lower state of (3). Thus a VB-based analysis of O_2 does correctly predict a triplet ground state. Early VB analyses[6] neglected the important role of the doubly-occupied π orbitals in arriving at a singlet ground state.

B.   Large R

At large R, we cannot assume that the p_z orbitals are paired into σ bond as in (2) and (3). Instead we must [for (3a)] take the $p_{y\ell}$ and $p_{z\ell}$ orbitals to be triplet-coupled and the p_{xr} and p_{zr} orbitals to be triplet-coupled. This allows us to form three states: a singlet, triplet, and quintet. In this case

an analysis of the exchange terms yields permutational numbers[13] of $+\frac{1}{2}$, 0, and -1 for the $p_{z\ell}$ and p_{zr} orbitals of the singlet, triplet, and quintet states, respectively, as compared with +1 for (3a). Thus at large R the singlet state should be lowest.

Clearly the permutational coupling changes significantly with R and variations in this quantity must be allowed.

In the Hartree-Fock method the permutational coupling is fixed; however, there are other even more serious limitations. Thus in the conventional HF wavefunction for the ground state of O_2 there are seven doubly-occupied and two singly-occupied orbitals at all internuclear separations. However, each ground state O atom has three doubly-occupied and two singly-occupied orbitals, leading hence to an excited description of the separated atoms.

The GVB approach is conceptually more consistent in that each electron can have a separate orbital. Thus, as the molecule is pulled apart, the orbitals can be equally distributed on the two centers. The GVB wavefunction for N electrons has the form

$$\psi_{GVB} = \mathcal{A} \left\{ [\, \phi_a(1)\phi_b(2) \cdots \phi_n(N)] \chi(1, 2, \cdots N) \right\}, \qquad (5)$$

where $\mathcal{A}$ is the antisymmetrizer. The spin function χ, which is an eigenfunction of $\hat{S}^2$, defines (through the antisymmetrizer) how the orbitals $\{\phi\}$ are coupled permutationally. Optimization of (5) consists of self-consistently determining the optimal set of orbitals and the optimal form of χ.[9,14]

Because of the complexity of spin eigenfunctions for many-electron systems, it is convenient to use diagrams to represent the ways in which various orbitals are permutationally coupled. The overall shape of a diagram indicates the number of electrons and the eigenstate of $\tilde{S}^2$ being considered. Internal partitions denote the specific coupling pattern involved. Two orbitals

placed horizontally within a rectangle are singlet-paired, and two or more orbitals placed vertically within a rectangle are coupled to high spin. The standard (linearly independent) couplings for four-electron singlets and triplets are given in Figure 1.

In O_2 at small R, we expect the two highly overlapping orbitals comprising the sigma bond to be singlet-paired. Taking the internuclear axis to coincide with the z-axis and ignoring the orbitals which are doubly-occupied for $R = \infty$, the wave functions for the $^1\Delta_g$ and $^3\Sigma_g^-$ states [from (3a)] are

$$\psi_{^1\Delta_g}(R_e) \;=\; \begin{array}{|c c|} \hline P_{z\ell} & P_{zr} \\ \hline P_{y\ell} & P_{xr} \\ \hline \end{array} \tag{6a}$$

$$\psi_{^3\Sigma_g^-}(R_e) \;=\; \begin{array}{|c c|} \hline P_{z\ell} & P_{zr} \\ \hline P_{y\ell} & \\ \cline{1-1} P_{xr} & \\ \cline{1-1} \end{array} \tag{6b}$$

where we have labeled the self-consistent orbitals according to their atomic origin. At large internuclear distances, however, the orbitals on each center must be coupled as in the ground state atom. Since ^3P oxygen atom has two singly-occupied orbitals triplet-coupled, the wavefunctions at large R are

$$\psi_{^1\Delta_g}(\infty) \;=\; \begin{array}{|c|c|} \hline P_{z\ell} & P_{zr} \\ \hline P_{y\ell} & P_{xr} \\ \hline \end{array} \tag{7a}$$

$$\psi_{^3\Sigma_g^-}(\infty) \;=\; \sqrt{\tfrac{2}{3}} \; \begin{array}{|c|c|} \hline P_{z\ell} & P_{zr} \\ \hline P_{y\ell} & \\ \cline{1-1} P_{xr} & \\ \cline{1-1} \end{array} \;+\; \sqrt{\tfrac{1}{3}} \; \begin{array}{|c|c|} \hline P_{z\ell} & P_{xr} \\ \hline P_{y\ell} & \\ \cline{1-1} P_{zr} & \\ \cline{1-1} \end{array} \tag{7b}$$

$$= \tfrac{1}{2}\mathcal{A}\,\{p_{z\ell}p_{y\ell}p_{zr}p_{xr}[\alpha\alpha(\alpha\beta + \beta\alpha) - (\alpha\beta + \beta\alpha)\alpha\alpha]\}\,.$$

Therefore, the simplest wavefunction capable of correctly describing dissociation of these states must be a linear combination of these atomic and molecular couplings

$$\Psi_{{}^1\Delta_g}(R) \;=\; C_m \;\boxed{\begin{array}{cc} p_{z\ell} & p_{zr} \\ \hline p_{y\ell} & p_{xr} \end{array}} \;+\; C_a \;\boxed{\begin{array}{c|c} p_{z\ell} & p_{zr} \\ p_{y\ell} & p_{xr} \end{array}} \tag{8a}$$

$$\mathrm{{}^3\Sigma_g^-}(R) \;=\; C_m \;\boxed{\begin{array}{cc} p_{z\ell} & p_{zr} \\ p_{y\ell} \\ p_{xr} \end{array}} \;+\; C_a\left\{\sqrt{\tfrac{2}{3}}\;\boxed{\begin{array}{c|c} p_{z\ell} & p_{zr} \\ p_{y\ell} \\ \hline p_{xr} \end{array}} \;+\; \sqrt{\tfrac{1}{3}}\;\boxed{\begin{array}{c|c} p_{z\ell} & p_{xr} \\ p_{y\ell} \\ p_{zr} \end{array}}\right\} \tag{8b}$$

The GVB wavefunction (5) for any R can always[15] be cast in the form of (8) [where the atomic labels of (8) serve only to identify the orbitals, they are no longer localized atomic orbitals].

III. CALCULATIONAL DETAILS

A. The Wavefunction

In the GVB method we can allow all orbitals to be singly-occupied; however the separated atoms each involve three doubly-occupied orbitals so that the minimal GVB description is to allow six doubly-occupied orbitals (four sigma and two pi) and four singly-occupied orbitals (two sigma and two pi). We found that splitting further pairs with GVB led to only minor effects and hence used this level of GVB [often denoted as GVB(2) indicating that all but four orbitals are doubly-occupied] throughout this paper.

As GVB calculations involving more than a very few electrons acquire immense computational complexity, two approximations are made in most GVB calculations. These approximations, which are actually restrictions, are perfect pairing and strong orthogonality.[10] The former approximation restricts the spin function in (6) to singlet couple as many orbital pairs as is possible for a given eigenstate of $\widehat{S}^2$. That is, for a state of spin S

$$\chi_{PP} = [\alpha(1)\beta(2) - \beta(1)\alpha(2)][\alpha(3)\beta(4) - \beta(3)\alpha(4)] \cdots \quad (9)$$

with the last 2S spins being α. The strong orthogonality restriction requires each orbital to be orthogonal to all other orbitals except for the other orbital in the same pair. As this perfect pairing (GVB-PP) wavefunction can be cast in a form requiring only simple HF-like variational equations for solution, GVB-PP calculations can easily be performed on relatively large numbers of electrons.[10]

While the perfect pairing restriction is often an excellent approximation, it is inadequate for cases where significant orbital coupling changes can be expected (e.g., chemical reactions). The case at hand clearly demonstrates this in that the GVB-PP wavefunctions (6) are unable to properly describe

dissociation. To overcome this limitation, the GVB equations were reformulated, removing the perfect pairing restriction, but maintaining the requirement of strong orthogonality (orbitals are still grouped into nonorthogonal pairs, but are not required to be coupled in any specific manner). As this strongly orthogonal (GVB-SO) wavefunction retains much of the computational simplicity of GVB-PP, it too can readily handle fairly large numbers of electrons.[11] Because of symmetry the orbitals of the GVB(2) wavefunction of O_2 satisfy the strong orthogonality condition and use of these programs leads to the (unrestricted) GVB wavefunction.

B.   Basis Set

The calculations were carried out using the double-zeta (DZ) basis set [4s2p] of Dunning,[16] contracted from the [9s5p] Gaussian set of Huzinaga,[17] and augmented by five uncontracted d-functions on each center, each having an exponent of 0.9.

This basis is often referred to as [4s2p1d] and denoted as DZd. The double-zeta set by itself is inadequate to describe the molecular bond formation, since with this basis the energy of the $^1\Delta_g$ state at 4 bohr is lower than that of both the $^3\Sigma_g^-$ and $^1\Delta_g$ states at R_e (see Table I).

IV.   RESULTS

A.   Orbitals and Orbital Coupling

The orbitals from the GVB calculations on the $^3\Sigma_g^-$ state are shown for various R in Figure 2. The orbitals for the $^1\Delta_g$ state are essentially the same. As expected, the 1s orbitals (not shown) and the 2s orbitals remain localized as the atoms are brought together. The $2p_z$ orbitals, which are paired to form a bond, do not change significantly until around $R = 4a_0 = 2.1$ Å. Because of the Pauli principle the $O_\ell 2p_z$ orbital must remain orthogonal to the $O_r 2s$ doubly-occupied orbital and this seems to be a dominant influence upon the changes in the shape of both orbitals. (Similar results of course apply to $O_r 2p_z$ and $O_\ell 2s$.) Orthogonalizing the $O_\ell 2p_z$ orbital to $O_r 2s$ would lead to just the type of character built up in $O_\ell 2p_z$ as R decreases. The way to decrease this effect on $O_\ell 2p_z$ is to hybridize the $O_r 2s$ orbital to the right (decreasing its overlap with $O_\ell 2p_z$) and by $R = 3a_0$ we already see such changes in $O_r 2s$. As the internuclear separation decreases, the overlap between the $2p_z$ orbitals continually increases, reaching a value of 0.24 at $R = 4a_0$ and a value of 0.80 at R_e.

At $R = 4a_0$, the four π orbitals are still basically atomic. Indeed, significant changes in these orbitals do not occur until around $3a_0$. At this point, the doubly-occupied $O_\ell 2p_x$ and $O_r 2p_y$ orbitals begin to delocalize in a bonding manner onto the other center. The singly-occupied $O_r 2p_x$ and $O_\ell 2p_y$ orbitals also delocalize, but do so in an antibonding manner in order to remain orthogonal to the doubly-occupied orbitals. By R_e, these orbitals are almost equivalently delocalized onto both centers.
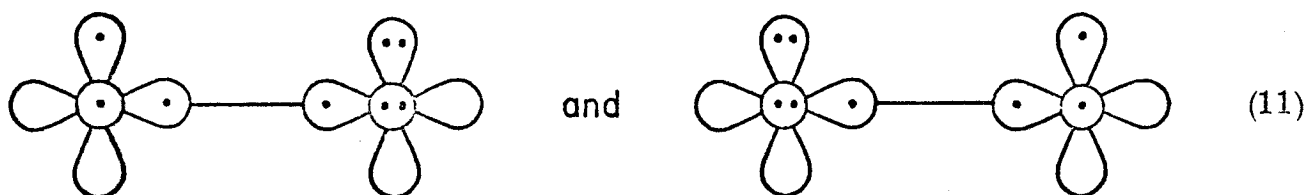
In the HF description the π orbitals are of π_u (bonding) and π_g (antibonding) symmetries. The GVB orbitals at R_e are close to this description, but

as R increases we see that the optimum orbitals become more and more localized. The problem in the HF description can be seen by expanding the π_{gx} and π_{gy} orbitals in terms of atomic components,

$$\pi_{gx}(1)\pi_{gy}(2) = (\ell_x + r_x)(\ell_y + r_y)$$

$$= (\ell_x \ell_y + r_x r_y) + (\ell_x r_y + r_x \ell_y). \tag{10}$$

$$\underbrace{}_{\text{ionic}} \quad \underbrace{}_{\text{covalent}}$$

Thus use of symmetry functions as in HF leads to equal amounts of ionic and covalent character in the wavefunction. Putting in the other π electrons shows that the HF wavefunction is a superposition of the covalent configurations (3a) and (3b) along with the ionic configurations

$$\tag{11}$$

(including the HF description of the σ bond leads to additional ionic configurations).

Changes in the coupling between the orbitals are also straightforward and in line with our qualitative expectations. Results of analysis of the GVB wavefunctions in terms of the atomic and molecular couplings of (9) are shown in Figure 3. As we see, concurrent with increasing overlap between the $2p_z$ orbitals, molecular coupling becomes of ever increasing importance as R is decreased from infinity to R_e. As expected, at R_e molecular coupling vastly predominates over any residual atomic coupling. Comparing these curves,

we note that the degree of 'molecular' coupling in the triplet always exceeds that of the singlet state. The reason for this is that while the exchange interactions between the singly-occupied π orbitals in (6b) are favorable, these same interactions are quite unfavorable in (6a). (This was the same reason used to conclude that the $^3\Sigma_g^-$, and not the $^1\Sigma_u^-$, was the ground state of O_2.)

The optimum orbitals for the $^3\Sigma_g^-$ state at R_e are grouped together in Figure 4.

B.   Spatial Symmetry and CI

In the GVB method we use a simple orbital product such as in (5) and optimize the orbitals and spin coupling. The result as shown in Figures 2 and 4 is to obtain orbitals localized more on the left or right side of the molecule. This is fine except that closer examination shows that this wavefunction corresponds to symmetry D_{2d} rather than $D_{\infty h}$. The origin of this difficulty can be spotted in (3a) and (3b), neither of which describes $D_{\infty h}$ symmetry. To obtain proper symmetry functions we must combine (3a) and (3b) as

$$(12)$$
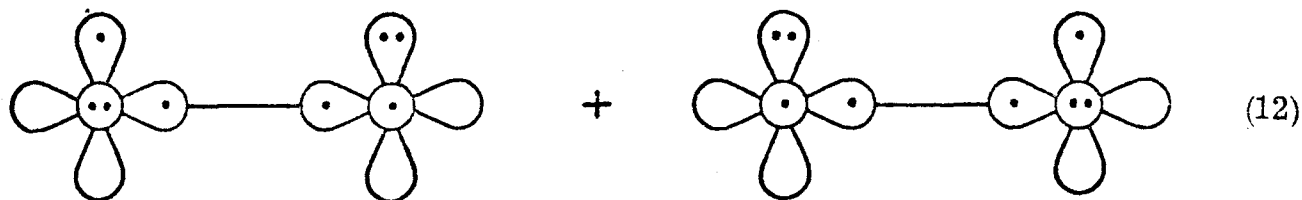
leading to $^1\Delta_g$ and $^3\Sigma_g^-$ states [use of a minus sign in (12) leads to $^1\Sigma_u^-$ and $^3\Delta_u$ states]. The GVB method has been extended[18] to allow for such spatial projection techniques (denoted as GVB-SP); however the calculations are expensive and the programs are not suitable for $D_{\infty h}$ symmetry. However, from previous experience the GVB-SP orbitals for O_2 are expected to be similar to the GVB orbitals and in this paper we have obtained wavefunctions of the proper

total symmetry by carrying out small configuration interaction (CI) calculations using the GVB orbitals.

These CI calculations were carried out as follows: The GVB orbitals corresponding to combinations of O1s and O2s orbitals on the atoms are denoted as $1\sigma_g$, $1\sigma_u$, $2\sigma_g$, and $2\sigma_u$; The GVB orbitals corresponding to the σ bond are combined into symmetry orbitals denoted as $3\sigma_g$ and $3\sigma_u$. The doubly-occupied π orbitals (both x and y) are combined into symmetry functions denoted as $1\pi_u$ and $2\pi_g$ and the singly-occupied π orbitals (both x and y) are combined into symmetry functions denoted as $2\pi_u$ and $1\pi_g$. The $2\pi_u$ and $2\pi_g$ orbitals obtained by this process are very similar to $1\pi_u$ and $1\pi_g$. For the CI calculations we obtain $2\bar{\pi}_u$ and $2\bar{\pi}_g$ orbitals by orthogonalizing to the $1\pi_u$ and $1\pi_g$ orbitals.

In terms of symmetry functions the GVB wavefunction has the form

$$\mathcal{A}\{\phi_{1\sigma_g}^2 \phi_{1\sigma_u}^2 \phi_{2\sigma_g}^2 \phi_{2\sigma_u}^2 (\phi_{3\sigma_g}^2 - \lambda_1 \phi_{3\sigma_u}^2)(\phi_{1\pi_{ux}}^2 \phi_{1\pi_{gx}} - \lambda_2 \phi_{1\pi_{gx}}^2 \phi_{1\pi_{ux}})$$

$$\times (\phi_{1\pi_{uy}}^2 \phi_{1\pi_{gy}} - \lambda_2 \phi_{1\pi_{gy}}^2 \phi_{1\pi_{uy}}) \chi\} \qquad (13)$$

(if we assume that $2\pi_u = 1\pi_u$ and $2\pi_g = 1\pi_g$). Expanding out (13) leads to the 12 terms above the line in Table II. [In (13) we assumed the molecular orbital coupling (6) and did not include the $(3\sigma_g)^1(3\sigma_u)^1$ term; for more general couplings these terms are required as noted in Table II.] Half the configurations in Table II have u symmetry and could be omitted for the g states. The remaining six spatial configurations would lead to a wavefunction quite close to the spatially projected GVB wavefunction, except for the slight restrictions we have made in the π orbitals ($2\pi_u = 1\pi_u$, $2\pi_g = 1\pi_g$). In order to allow for readjustments in these π orbitals we allowed single excitations from the 12 configurations of Table II (above the line) into the $2\bar{\pi}_u$ and $2\bar{\pi}_g$ orbitals. In order to allow for readjustments in the orbitals due to the presence of spatial projection terms,

we allowed a full CI among the eight valence orbitals.

The GVB wavefunction for the states corresponding to (2a) and (2b) leads to the 18 configurations below the line (12 of g symmetry). In order to describe all the low-lying states of O_2 with a CI compatible with a spatially projected GVB wavefunction, we added these 18 to the above 12 and carried out similar types of excitations. The result was 72 configurations for $^3\Sigma_g^-$ and 98 configurations for $^1\Delta_g$ or $^1\Sigma_g^+$. Later we will report a study of a number of additional excited states of O_2 using this set of configurations.

C.   Energies

The energies from the GVB calculations are tabulated in Table I and plotted in Figure 5, where we see that the GVB wavefunctions do behave properly, leading to ground state O atoms as the bond is stretched to infinity. This is in clear contrast to the HF and GVB-PP curves which do not exhibit this correct behavior at large R. At R_e, the $^1\Delta_g$ - $^3\Sigma_g^-$ separation is 0.87 eV, in good agreement with experiment (1.01 eV).[19] However, there is little point in dwelling upon these curves since they do not include the spatial projection effects. It is, rather, the potential curves obtained from the CI calculations using the GVB orbitals that are of importance.

The CI results are reported in Table I and plotted in Figure 4. The calculated values for the bond distance (R_e), bond energy (D_e), and vibrational frequency (ω_e) are listed in Table II and compared with experimental results. Thus these calculations account for 92.9% of the bond energy and lead to an R_e too large by 1.7%. For comparison, Schaefer[20] carried out "first-order" CI calculations on the $^3\Sigma_g^-$ state obtaining 90.6% of the bond energy and an R_e 1.1% too large.

The excellence of these CI results suggests to us that the GVB orbitals contain the essential features of these states of O_2 and hence that the concepts developed here and based on these orbitals are valid.

TABLE I. Energies from GVB and GVB-CI calculations on O_2 using the DZd basis. (Add the quoted number to -149. to obtain the total energies in hartrees).

Internuclear Distance (a_0)	$^3\Sigma_g^-$		$^1\Delta_g$	
	GVB	GVB-CI	GVB	GVB-CI
2.0	-0.62241	-0.71401	-0.57513	-0.66951
2.285616[a]	-0.65978	-0.78030	-0.62773	-0.73923
2.5	-0.64978	-0.77278	-0.63437	-0.73559
3.0	-0.61954	-0.70471	-0.62084	-0.67998
3.5	-0.60156	-0.64204	-0.60821	-0.63387
4.0[a]	-0.59847	-0.61167	-0.60353	-0.61346
4.5	-0.59976	-0.60480	-0.60210	-0.60665
5.0	-0.60064	-0.60362	-0.60155	-0.60433
6.0	-0.60107	-0.60313	-0.60118	-0.60298

[a]With the DZ basis the GVB energies of the $^3\Sigma_g^-$ and $^1\Delta_g$ states are -149.60154 and -149.54193 at 2.285616 a_0 and -149.59797 and -149.60301 at 4.0 a_0.

TABLE II. Parameters of the potential curves of O_2 from the GVB-CI calculations.

| | $^3\Sigma_g^-$ | | $^1\Delta_g$ | |
	Calc.	Exp.[a]	Calc.	Exp.[a]
R_e (Å)	1.238	1.208	1.249	1.216
D_e (eV)	4.88	5.21	3.79	4.23
ω_e (cm^{-1})	1693.	1580.	1595.	1509.
ΔE (eV)	-	-	1.09	1.01

[a] Experimental values are from Ref. 19.

TABLE III. Basic configurations for GVB-CI (the $1\sigma_g$ and $1\sigma_u$ orbitals are doubly-occupied).

$2\sigma_g$	$2\sigma_u$	$3\sigma_g$	$3\sigma_u$	$1\pi_{ux}$	$1\pi_{gx}$	$1\pi_{uy}$	$1\pi_{gy}$	Inversion Symmetry
2	2	2	0	2	1	2	1	g
2	2	2	0	2	1	1	2	u
2	2	2	0	1	2	2	1	u
2	2	2	0	1	2	1	2	g
2	2	1	1	2	1	2	1	u
2	2	1	1	2	1	1	2	g
2	2	1	1	1	2	2	1	g
2	2	1	1	1	2	1	2	u
2	2	0	2	2	1	2	1	g
2	2	0	2	2	1	1	2	u
2	2	0	2	1	2	2	1	u
2	2	0	2	1	2	1	2	g
2	2	2	0	2	2	2	0	g
2	2	2	0	2	2	1	1	u
2	2	2	0	2	2	0	2	g
2	2	2	0	2	0	2	2	g
2	2	2	0	1	1	2	2	u
2	2	2	0	0	2	2	2	g
2	2	1	1	all six cases				
2	2	0	2	all six cases				

REFERENCES

1. Partially supported by a grant (GP-40783X) from the National Science Foundation.

2. National Science Foundation Trainee, 1970-71; ARCS Foundation Fellow, 1971-73; Woodrow Wilson Fellow, 1972; National Science Foundation Fellow, 1972-73. Present address: Battelle Memorial Institute, 505 King Avenue, Columbus, Ohio 43201.

3. Contribution No.

4. R. S. Mulliken, Phys. Rev. 32, 880 (1928).

5. G. Herzberg, Spectra of Diatomic Molecules (Van Nostrand, New York, 1950).

6. W. Heitler and G. Nordheim-Poschl, Nature 133, 833 (1934).

7. W. A. Goddard III and R. C. Ladner, J. Amer. Chem. Soc. 93, 6750 (1971).

8. W. A. Goddard III, T. H. Dunning, Jr., W. J. Hunt, and P. J. Hay, Accts. Chem. Res. 6, 368 (1973).

9. R. C. Ladner and W. A. Goddard III, J. Chem. Phys. 51, 1073 (1969).

10. R. C. Ladner, Ph.D. Thesis, California Institute of Technology, November 1971.

11. F. W. Bobrowicz, Ph.D. Thesis, California Institute of Technology, 1974.

12. W. A. Goddard III, P. J. Hay, and T. H. Dunning, Jr., J. Amer. Chem. Soc., submitted for publication.

13. C. W. Wilson, Jr., and W. A. Goddard III, Theor. Chim. Acta 26, 195, 211 (1972).

14. Optimization of χ has previously also been referred to as spin-coupling optimization[9] or simply spin-optimization.

15. For four electron triplets there are generally three linearly independent spin couplings, but the third vanishes by symmetry for this state of O_2.

16. T. H. Dunning, Jr., J. Chem. Phys. 53, 2823 (1970).

17. S. Huzinaga, J. Chem. Phys. 42, 1293 (1965).

18. G. Levin and W. A. Goddard III, Chem. Phys. 4, 409 (1974); idem, Theor. Chim. Acta, submitted for publication; G. Levin, Ph.D. Thesis, California Institute of Technology, April 1974.

19. P. Krupenie, J. Phys. Chem. Ref. Data 1, 423 (1972).

20. H. F. Schaefer III, J. Chem. Phys. 54, 2207 (1971).

FIGURE CAPTIONS

Figure 1.   Standard couplings for four-electron systems.

Figure 2.   GVB orbitals for O_2 as a function of internuclear distance. Long dashed lines indicate zero amplitude. Solid and short dashed lines indicate positive and negative amplitude. Spacing between successive contours is 0.05 a.u.

Figure 3.   GVB orbital coupling coefficients for O_2 as a function of internuclear distance. They have been normalized so that $|C_m| + |C_a| = 1$ and $C_m \geq 0$.

Figure 4.   The GVB orbitals for the $^3\Sigma_g^-$ state at R_e.

Figure 5.   Potential energy curves for the $^3\Sigma_g^-$ and $^1\Delta_g$ states of O_2 from HF, GVB-PP, GVB, and GVB-CI calculations.

FOUR-ELECTRON SINGLET

G1

$$\boxed{\begin{array}{cc}\phi_i & \phi_j \\ \phi_k & \phi_\ell\end{array}} = \tfrac{1}{2}\mathcal{A}\{\phi_i\phi_j\phi_k\phi_\ell(\alpha\beta\alpha\beta - \alpha\beta\beta\alpha - \beta\alpha\alpha\beta + \beta\alpha\beta\alpha)\}$$

G2

$$\boxed{\begin{array}{c|c}\phi_i & \phi_k \\ \phi_j & \phi_\ell\end{array}} = \frac{1}{\sqrt{12}}\mathcal{A}\{\phi_i\phi_j\phi_k\phi_\ell(2\alpha\alpha\beta\beta - \beta\alpha\beta\alpha - \alpha\beta\beta\alpha - \alpha\beta\alpha\beta + 2\beta\beta\alpha\alpha - \beta\alpha\alpha\beta)\}$$

FOUR-ELECTRON TRIPLET

G1

$$\begin{array}{cc}\phi_i & \phi_j \\ \phi_k \\ \phi_\ell\end{array} = \frac{1}{\sqrt{2}}\mathcal{A}\{\phi_i\phi_j\phi_k\phi_\ell(\alpha\beta\alpha\alpha - \beta\alpha\alpha\alpha)\}$$

G2

$$\begin{array}{c|c}\phi_i & \phi_k \\ \phi_j \\ \phi_\ell\end{array} = \frac{1}{\sqrt{6}}\mathcal{A}\{\phi_i\phi_j\phi_k\phi_\ell(2\alpha\alpha\beta\alpha - \alpha\beta\alpha\alpha - \beta\alpha\alpha\alpha)\}$$

G3

$$\begin{array}{c|c}\phi_i & \phi_\ell \\ \phi_j \\ \phi_k\end{array} = \frac{1}{\sqrt{12}}\mathcal{A}\{\phi_i\phi_j\phi_k\phi_\ell(3\alpha\alpha\alpha\beta - \beta\alpha\alpha\alpha - \alpha\beta\alpha\alpha - \alpha\alpha\beta\alpha)\}$$

Fig. 1.

(a) O₂ SIGMA ORBITALS (GVB)

SIGMA BOND PAIR

Oₗ 2s PAIR · · · Oₗ 2pz · · · Oᵣ 2pz · · · Oᵣ 2s PAIR

R = 4.00a₀

R = 3.00a₀

R = 2.28a₀

PAIRED

Z · · · Z · · · Z · · · Z

X · · · X · · · X

3.0

-3.0

-4.0 · · · 4.0

Fig. 2a
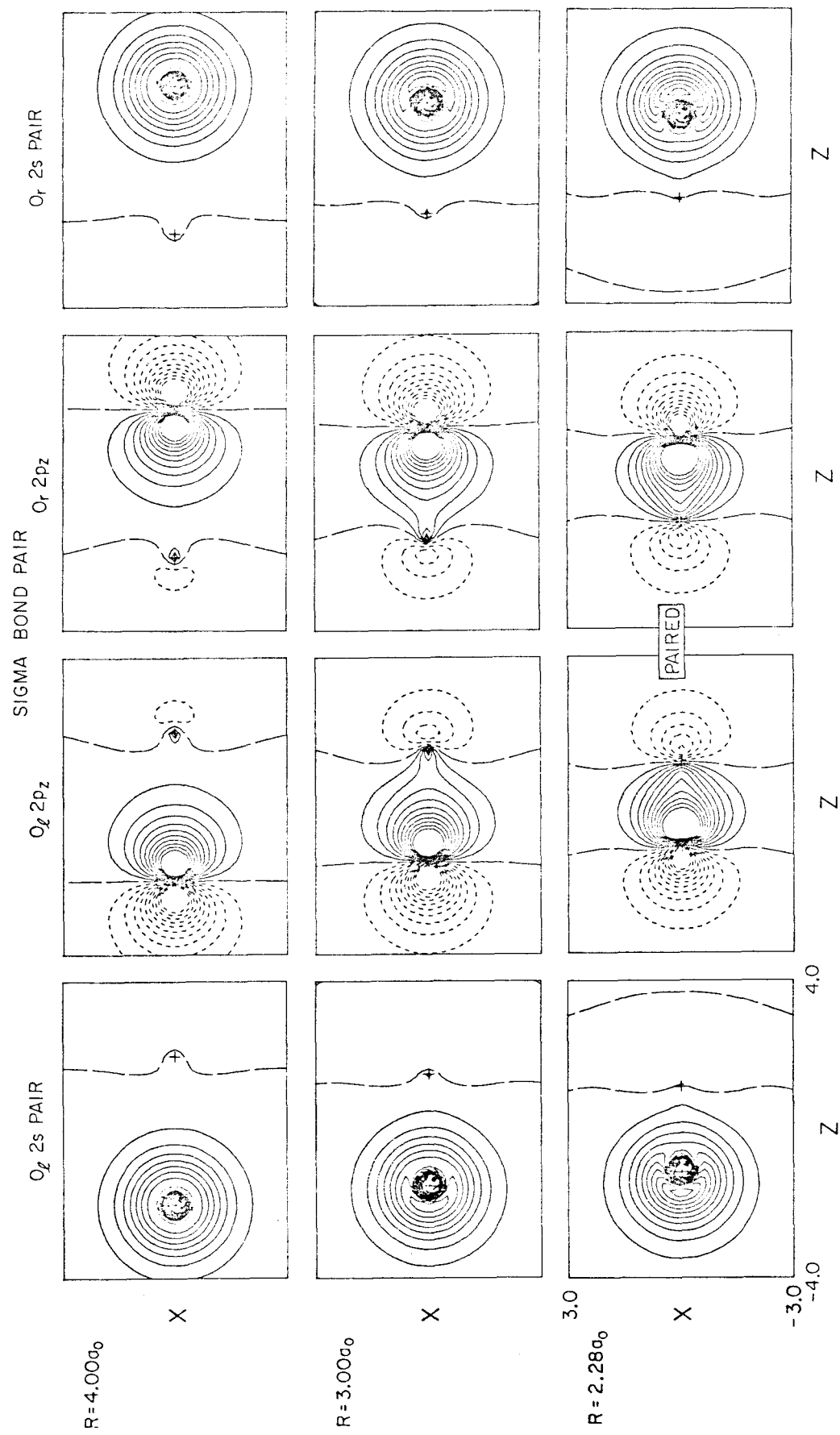
(b) O₂ PI ORBITALS (GVB)

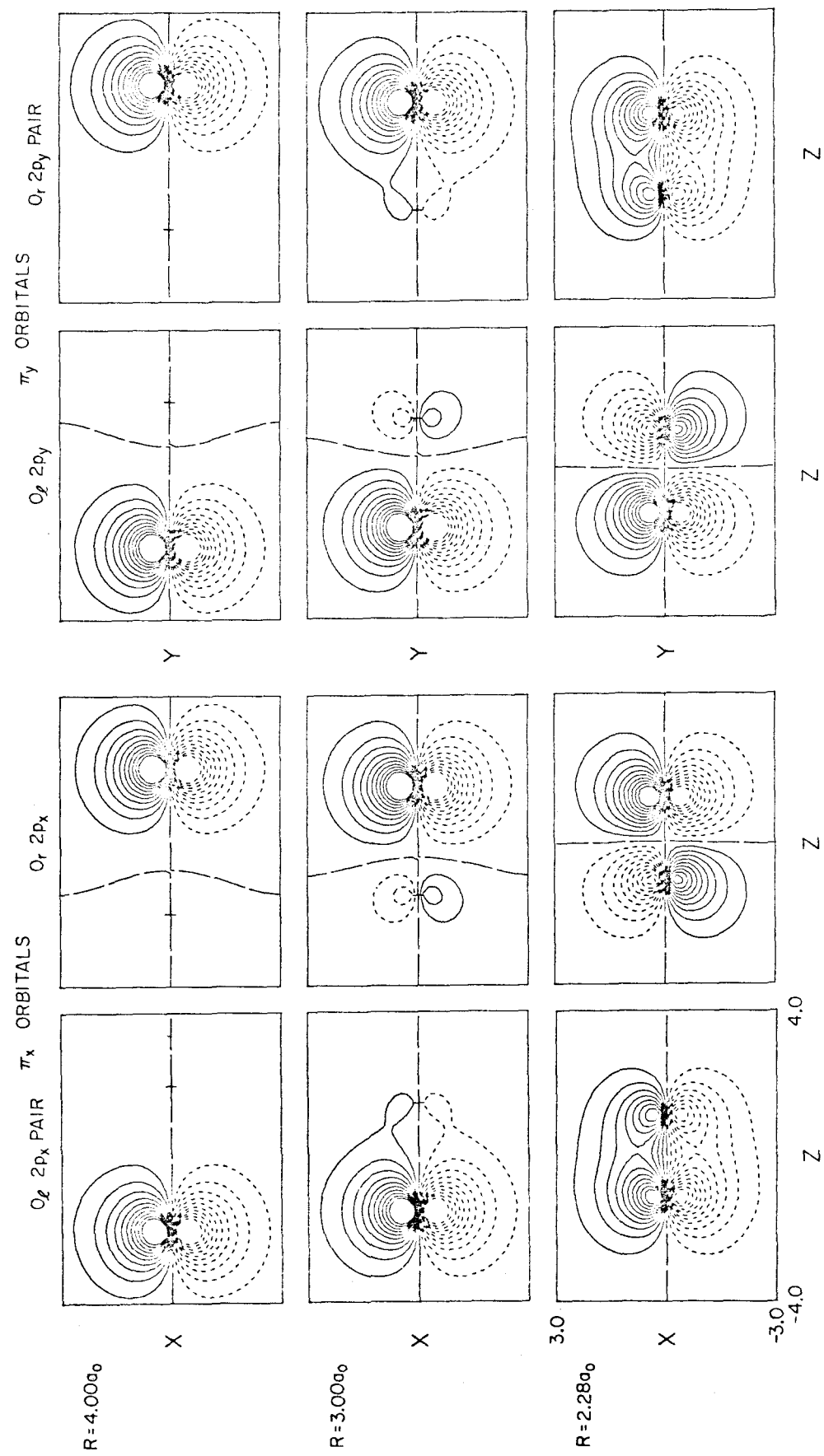Fig. 2b

Fig. 3

GVB ORBITALS

$O_2(X^3\Sigma_g^-)$

LEFT CENTER · RIGHT CENTER

O_ℓ 2s PAIR · O_r 2s PAIR

O_ℓ 2p_z · O_r 2p_z · PAIRED

O_ℓ 2p_x PAIR · O_r 2p_x

O_ℓ 2p_y · O_r 2p_y PAIR

3.0 · -3.0 · -4.0 · Z · 4.0 · Z · X · Y
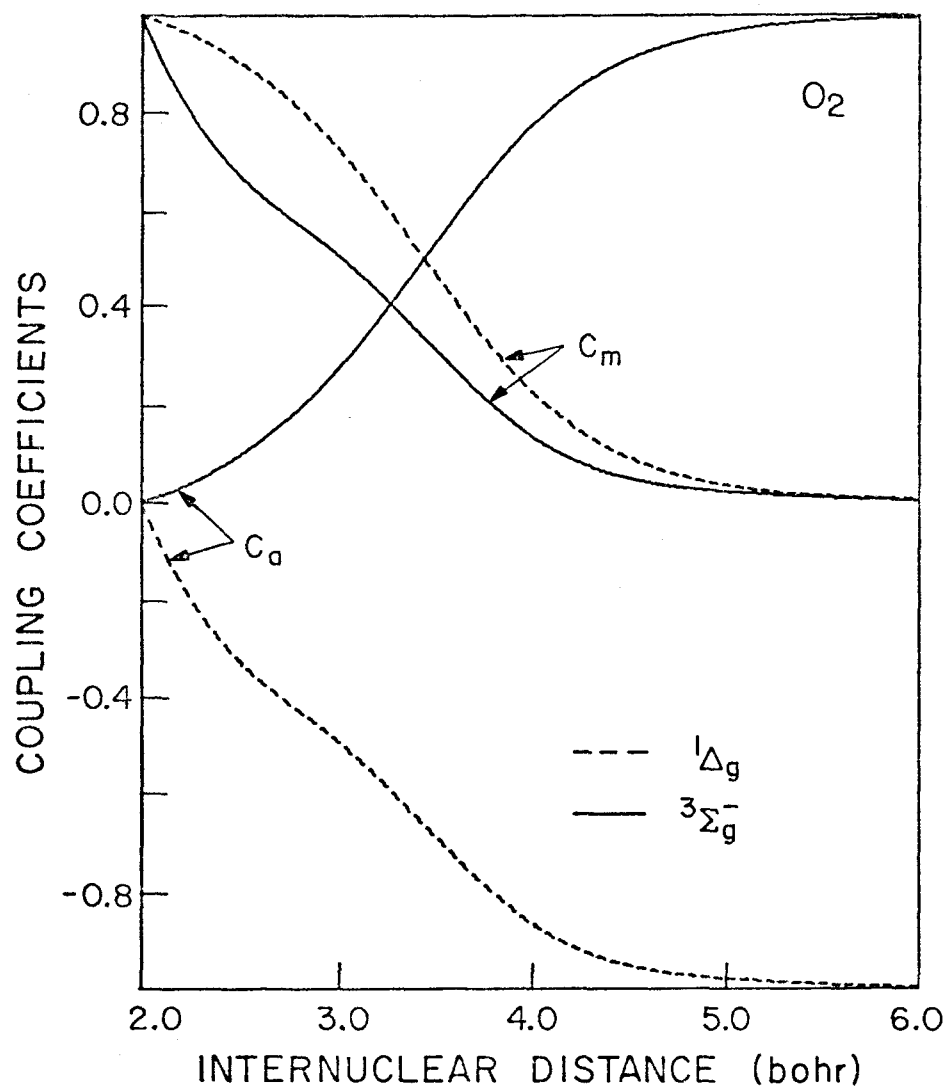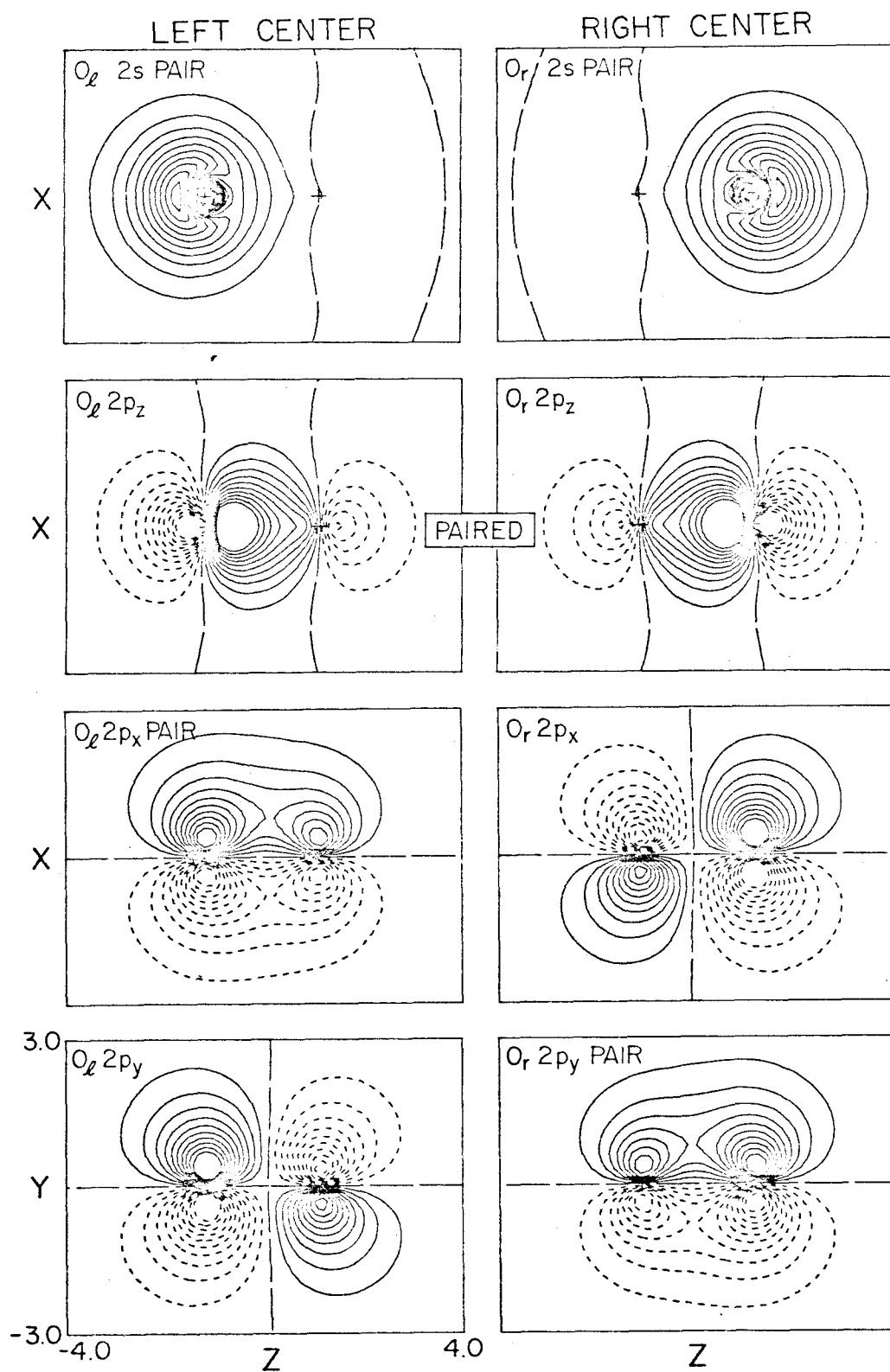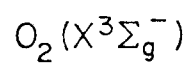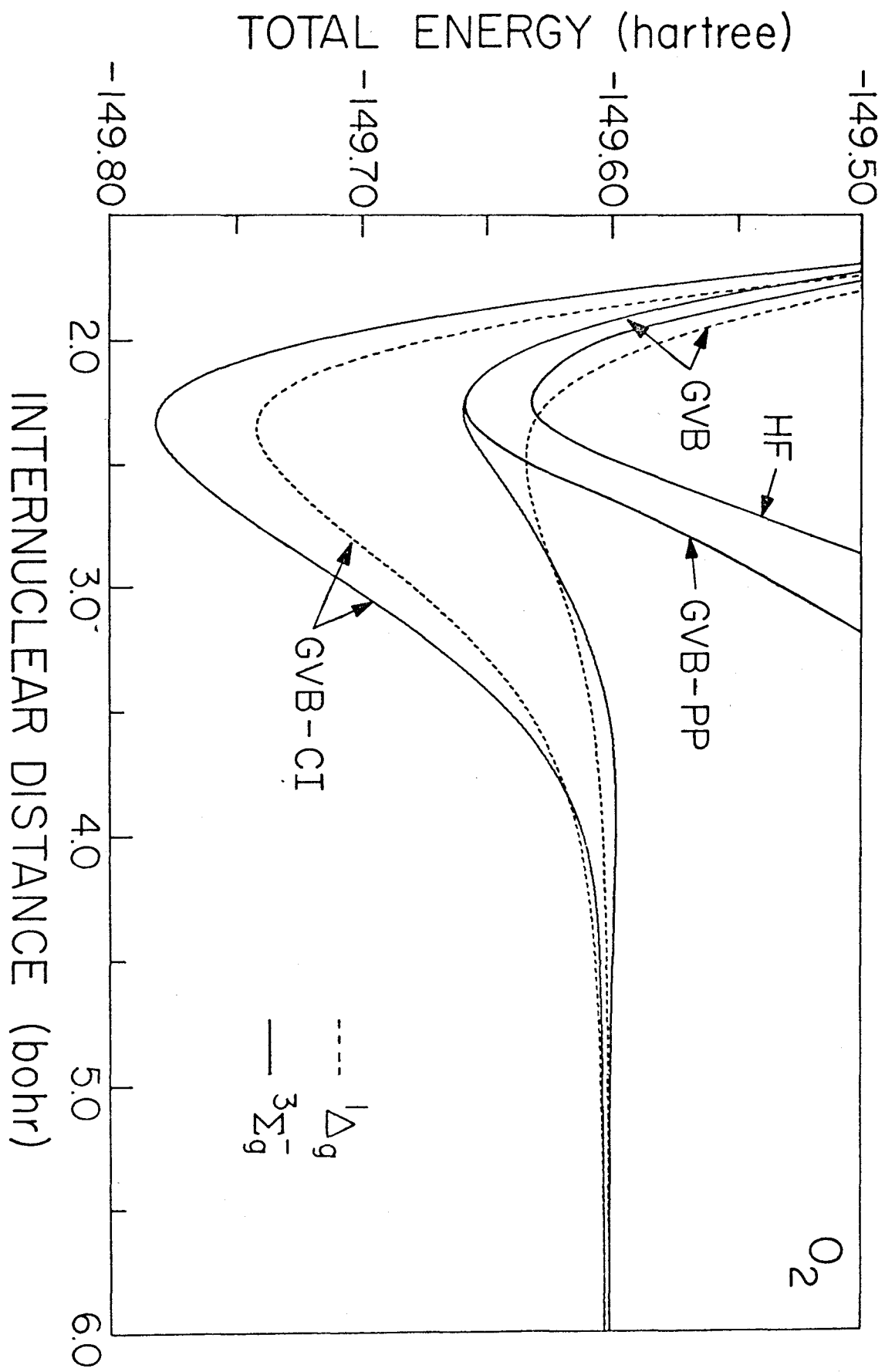
Fig. 4

Fig. 5

PART TWO:

Configuration Interaction Studies on Low-Lying States of O_2

I. INTRODUCTION

The first great success of MO theory was the rationalization of the paramagnetic behavior of the ground state and the prediction of the low-lying excited states.[2] However, full Hartree-Fock (HF) wavefunctions[12c] of O_2 account for only 1.43 eV out of 5.21 eV of the bond energy (besides providing a potential curve going to the wrong limits as the internuclear distance $R \rightarrow \infty$). On the other hand, for a basis adequate for describing dissociation (double zeta plus d polarization functions) a full configuration interaction (CI) calculation would involve $\sim 10^{12}$ determinants and just including all single and double excitations from the dominant configurations of the states being examined here ($\pi_u^4 \pi_g^2$ and $\pi_g^3 \pi_u^3$) would lead to ~ 2000 configurations, without excitation from the $1\sigma_g$ and $2\sigma_g$ orbitals. Thus studying a number of states of O_2 would lead to considerable expense.

In this paper we use the generalized valence bond (GVB) orbitals[3,4] for the carrying out of the CI calculations. Since the GVB wavefunction leads to the correct description of the wavefunction as $R \rightarrow \infty$ the CI wavefunctions are expected to be adequate even for large R. The excitation energies for small R are accurate to about 0.1 eV while the bond lengths are generally about 0.02 Å too long.

The calculational details are presented in Section II. A qualitative description of the wavefunctions in terms of GVB diagrams is given in Section III, followed in Section IV by an analysis of the corresponding configurations for the CI calculations. The results and discussions are presented in Section V.

II. CALCULATIONAL DETAILS

The basis set used in these studies is the double zeta basis of contracted Gaussians from Dunning[5] and Huzinaga, supplemented by a set of d basis functions on each oxygen (orbital exponent $\alpha = 0.9$). Such a basis is expected to yield a good description of the potential curves for valence states.

As shown previously[3] the orbital permutational coupling (also called spin coupling) must be allowed to vary with R, in order to obtain the proper description of dissociation. Thus the perfect pairing restrictions are unsuitable here, and they are not imposed. These GVB wavefunctions for O_2 are described elsewhere.[3]

The CI calculations were carried out with the Caltech CI program.[6]

III. QUALITATIVE DESCRIPTION

Ignoring the O1s and O2s orbitals for the moment, the oxygen atom may be pictured as
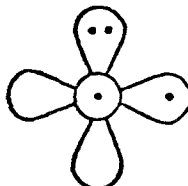
(1)

where $\bigcirc\!\!\!\bigcirc$ and $\bigcirc$ represent p orbitals parallel and perpendicular to the plane of the paper and the dots indicate the occupation.[4] Combining such configurations in the two atoms so as to describe a sigma bond between them leads to
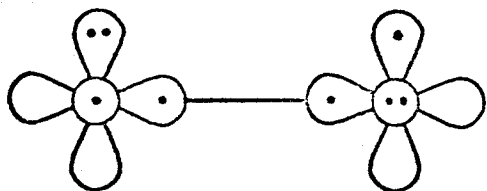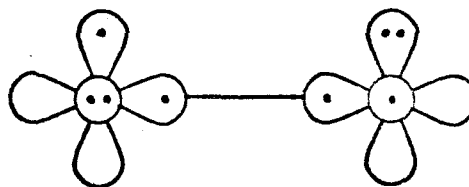
(2a)
(2b)

and
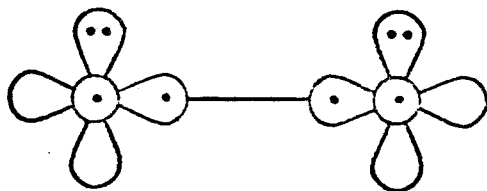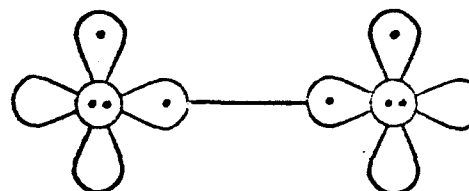
(3a)
(3b)

where the line indicates singlet pairing of the connected orbitals. Each configuration in (2) and (3) leads to both a singlet and a triplet state depending on the coupling of the singly-occupied π orbitals. The overall symmetries obtained with (2) and (3) are:

$$
\begin{aligned}
&\text{(2a)}: \quad {}^3\Sigma_g^- , \quad {}^1\Delta_g \\
&\text{(2b)}: \quad {}^1\Sigma_u^- , \quad {}^3\Delta_u \\
&\text{(3a)}: \quad {}^1\Sigma_g^+ , \quad {}^3\Sigma_u^+ \\
&\text{(3b)}: \quad {}^1\Delta_g , \quad {}^3\Delta_u
\end{aligned}
$$

(4)

(the two components of each Δ state appear separately).

As would be expected from (2) and (3) the states in (4) all go to the limit of two ground state (${}^3P$) oxygen atoms as $R \rightarrow \infty$. However, for small R they partition into two groups:

$$^3\Sigma_g^-, \quad {}^1\Delta_g, \quad \text{and} \quad {}^1\Sigma_g^+ \tag{5}$$

with large bond energies (3.5 to 5.2 eV) and

$$^1\Sigma_u^-, \quad {}^3\Delta_u, \quad \text{and} \quad {}^3\Sigma_u^+ \tag{6}$$

with small bond energies (0.8 to 1.1 eV). In this VB description these

states (5) and (6) just correspond to the resonant and antiresonant

combinations, respectively, of the four component configurations,

$$\tag{7}$$
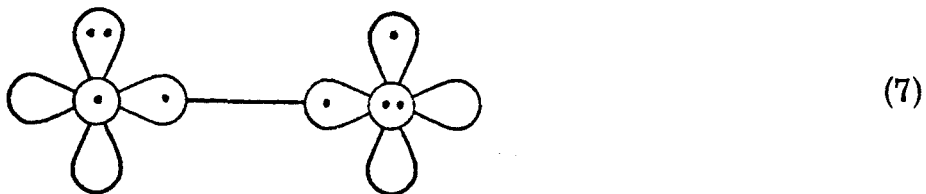
etc.

In the MO description[7] the lowest configuration is

$$(1\sigma_g)^2 \, (1\sigma_u)^2 \, (2\sigma_g)^2 \, (2\sigma_u)^2 \, (3\sigma_g)^2 \, (1\pi_u)^4 \, (1\pi_g)^2 \tag{8}$$

leading to the states in (5). The first excited configuration is

$$(1\pi_u)^3 \, (1\pi_g)^3 \tag{9}$$

(the σ occupations are unchanged) leading to

$$^3\Sigma_u^-, \quad {}^1\Delta_u, \quad {}^1\Sigma_u^+ \tag{10}$$

and the states in (6). Thus the resonant valence bond states (5) correspond

to the ground MO configuration while its antiresonant valence bond states

(6) correspond to half of the states of the first excited MO configuration.

Higher valence bond states are obtained with configurations such as

$$\text{(11a)}$$
$$\text{(11b)}$$
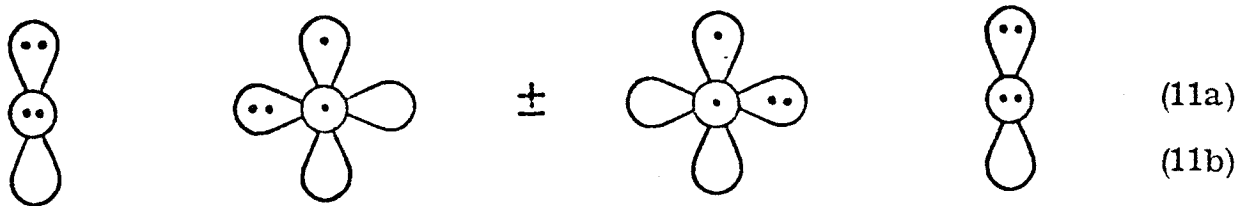
involving an excited state at $R = \infty$. Configuration (11b) gives rise to the

${}^{3}\Sigma_{u}^{-}$ and ${}^{1}\Delta_{u}$ states of (10) leading at $R = \infty$ to $O({}^{1}D) + O({}^{3}D)$ for ${}^{3}\Sigma_{u}^{-}$

and $O({}^{1}D) + O({}^{1}D)$ for ${}^{1}\Delta_{u}$. The other configuration (11a) leads to states

$(2\,{}^{3}\Sigma_{g}^{+},\ 2\,{}^{1}\Delta_{g})$ that at small R correspond to the

$$(1\,\pi_{u})^{2}\,(1\,\pi_{g})^{4} \tag{12}$$

MO configurations (that is, doubly-excited states).

IV. THE CI CALCULATIONS

The GVB calculations were carried out for the triplet and singlet states corresponding to the configurations in (7). This led to doubly-occupied $1\sigma_g$ and $1\sigma_u$ orbitals corresponding closely to combinations of the O1s orbitals and $2\sigma_g$ and $2\sigma_u$ orbitals corresponding closely to combinations of the O2s orbitals. The sigma bond pair of (7) can be written in terms of natural orbitals as

$$(\phi_{\sigma_\ell} \phi_{\sigma_r} + \phi_{\sigma_r} \phi_{\sigma_\ell}) = (\phi_{3\sigma_g} \phi_{3\sigma_g} - \lambda \phi_{3\sigma_u} \phi_{3\sigma_u}) \qquad (13)$$

(requiring normalization). The pi orbitals of (7) are localized but are combined into symmetry functions for the CI, leading to two sets of π_u orbitals and two sets of π_g orbitals. These combinations were taken so that $1\pi_u$ corresponds to a symmetry-projected doubly-occupied orbital while $1\pi_g$ corresponds to a symmetry-projected singly-occupied orbital. The $2\pi_g$ and $2\pi_u$ orbitals each correspond to the other possible projection but Schmidt-orthogonalized to $1\pi_g$ and $1\pi_u$.

In terms of symmetry functions (2) leads to the 12 configurations of Table Ia, and (3) leads to the 18 configurations of Table Ib. Carrying out the CI over these configurations leads to a close approximation to the GVB wavefunction (as discussed in more detail below) except that the orbitals are obtained from calculations on the $^3\Sigma_g^-$ state and hence need not be optimum for the other states. In addition the procedure of symmetrizing the GVB orbitals leads also to $2\pi_g$ and $2\pi_u$ orbitals omitted in Table I. To remedy these two effects we have included all single excitations from the valence orbitals of the 30 configurations in Table I, allowing the $2\pi_g$ and $2\pi_u$ orbitals to also be occupied. In addition we have included all

configurations involving various occupations of the eight valence orbitals of Table I. This leads, for example, to 98 configurations and 360 determinants for the $^1\Sigma_g^+$ state and 72 configurations and 224 determinants for the $^3\Sigma_g^-$ state. In contrast, a full CI among these 14 orbitals would involve about 10^6 determinants. This approach (exciting from all configurations required for describing the various states at R = ∞) is necessary to obtain a consistent treatment of the various states for all R.

V. RESULTS

The calculated potential curves are shown in Fig. 1, and a summary of relevant quantities is given in Table II. The calculated energies are tabulated in Table III.

A. Small R

The calculated dissociation energy for the ground state is $D_e = 4.88$ eV which is 93% of the exponential value,[7-9] 5.21 eV. The calculated excitation energies to the six experimentally known excited states of Table I are off by 0.11, 0.06, -0.16, -0.13, -0.14, and 0.13 eV respectively, an average error of 0.12 eV.

The calculated bond lengths for the lowest seven states are calculated to be 0.030, 0.033, 0.033, 0.008, 0.022, 0.007, and 0.021 Å longer than the experimental values. Using a cubic spline fit to obtain the calculated ω_e leads to values about 5 to 7% higher than the experimental ω_e for the first six states and about 6% too low for $B\,^3\Sigma_u^-$.

The error in the calculated dissociation energies is 0.4 eV for the states in (5), 0.2 eV for the states in (6) and 0.2 eV for $B\,^3\Sigma_u^-$. Thus the error is 0.4 eV for states with $R_e \approx 1.2$ Å and 0.2 eV for states with $R_e \approx 1.6$ Å, a reasonable result since the correlation errors should decrease exponentially with R. Assuming a similar 0.2 eV error in the calculated D_e for $^1\Delta_u$ and $^1\Sigma_u^+$ (both with $R_e \sim 1.65$ Å) leads to a predicted T_e of 8.4 eV for $^1\Delta_u$ and 10.3 eV for $^1\Sigma_u^+$.

There has been some difficulty[7,19,20] in establishing the T_e for the transitions to the $c\,^1\Sigma_u^-$, $C\,^3\Delta_u$ and $A\,^3\Sigma_u^+$ states due to difficulty in establishing the vibrational numbering in the observed transitions. The numbering in the $A\,^3\Sigma_u^+$ state seems, however, to finally be established[19] although the $c\,^1\Sigma_u^-$ and especially the $C\,^3\Delta_u$ states are uncertain.[20] Using the present numbering

schemes yields energy separations[7] of 0.21 and 0.08 eV for c–C and C–A in good agreement with our calculated values of 0.24 and 0.08 eV (vibrational spacings are ~0.1 eV). Thus our results indicate that the vibrational numbering of the $c^1\Sigma_u^-$ and $C^3\Delta_u$ states has been correctly assigned (assuming $A^3\Sigma_u^+$ to be correct).

No direct measurements are available for the vertical excitation energies for the $^1\Sigma_u^-$ and higher states (although indirect evidence[10] favors the $B^3\Sigma_u^-$ state as lying around 8.5 eV). Careful absorption measurements[18] indicate that the maximum for the $A^3\Sigma_u^+ \leftarrow X^3\Sigma_g^-$ absorption is >5.90 eV (the threshold for $B^3\Sigma_u^- \leftarrow X^3\Sigma_u^-$ is at 6.05 eV), a value consistent with our results.

These results indicate that our potential curves are reliable approximations to the exact potential curves for these states.

Previous accurate calculations on the $X^3\Sigma_g^-$ and $B^3\Sigma_u^-$ states have been reported by Schaefer[12] using "first order" CI wavefunctions. For the B state he finds a D_e of 0.76 eV and an R_e of 1.64 Å. For the X state he finds a D_e of 4.72 eV and an R_e of 1.22 Å.

Ohno and co-workers[13] suggested that the $B^3\Sigma_u^-$ state is diffuse but a later study by Morokuma[24] showed that it is not -- a result in agreement with our studies and that of Schaefer.[12]

B. Large R

Except for $B^3\Sigma_u^-$, there currently is no reliable experimental information on the potential curves for these states for $R > 2$ Å. There are interesting crossings in the first six states in the region of $3\frac{1}{2}$ to $6\,a_0$ as shown in Fig. 2, and we will examine here some of the reasons for this behavior.

Of these six states only $^3\Sigma_u^+$ is found to have a hump in the potential curve (calculated value 0.32 mh = 0.0087 eV). For $R > 4.5\,a_0$ the $^1\Sigma_u^-$

is found to be the lowest state. Given these variations, we would expect significant differences in the cross sections for formation of O_2 in the various states

$$O + O + M \rightarrow O_2^* + M .$$ (14)

It should be possible to use our results to calculate[16] approximate rate constants for these processes and it should be possible to design experimental methods[17] of distinguishing between the various processes. With such studies one may get a better understanding of the mechanisms of forming molecules in excited states and hence in some of the processes involved in gas discharges, flames, chemical lasers and in the upper atmosphere.

For $R \sim 6\, a_0$ we find that the three triplet states are equally spaced as are the singlet states (both about 0.12 mh) but that the singlet states are about one step below the triplet states, leading to four groups, $^1\Sigma_u^-$ lowest, $^3\Sigma_g^-$ and $^1\Delta_g$ next, $^3\Delta_u$ and $^1\Sigma_g^+$ next and $^3\Sigma_u^+$ highest.

This pattern of evenly spaced levels can be understood as follows: Assuming that the overlap of orbitals on different centers is zero, we coupled the orbitals as in (2) and (3) except that the singly-occupied orbitals on each center are taken as triplet paired (as a result the p_z orbitals opposite centers are no longer singlet paired). This leads to a spacing of the triplet levels by

$$\epsilon_1 \equiv 2[y_\ell x_\ell | y_r x_r]$$ (15)

which with atomic orbitals (at $6\, a_0$) is $\epsilon_1 = 0.1174$ mh. The corresponding calculation for the singlet states leads to

$$E(^1\Delta_g) - E(^1\Sigma_u^-) = \epsilon_1 + [y_r x_\ell | x_r y_\ell] + [y_r y_\ell | x_r x_\ell]$$ (16a)

$$E(^1\Sigma_g^+) - E(^1\Delta_g) = \epsilon_1 + [y_r x_\ell | x_r y_\ell]$$ (16b)

which with atomic orbitals (at 6 a_0) leads to 0.1208 mh and 0.1176 mh, respectively. Although this simple approximation accounts for these spacings correctly, it does not lead to the proper spacing between singlet and triplet states; the average of the singlet states should be 0.18 mh below the triplet states rather than 0.15 mh above them as calculated with zero overlap[21] (at 6 a_0 the overlap of atomic $p\pi$ orbitals is 0.003 while the overlap of atom $p\sigma$ orbitals is 0.023).

C. Analysis of the CI wavefunctions

In order to indicate the relative importance of configurations for the various states we have calculated the energy contribution of each configuration using the formula

$$\Delta E_\mu = C_\mu^2 (E - H_{\mu\mu})/(1 - C_\mu^2) . \qquad (17)$$

This corresponds to the energy increase that would occur if configuration μ is deleted while keeping all other CI coefficients fixed. In the case of several spin eigenfunctions corresponding to one spatial configuration we have merely added the separate contributions. Although the ΔE_μ serve to indicate the important configurations, the total energy is not the sum of ΔE_μ; for the dominant configurations the resulting ΔE_μ is of little significance.

Table IV shows the important configurations for the $X^3\Sigma_g^-$ state for various R. All configurations with $\Delta E_\mu > 1$ mh at R are included. The configurations occurring in an expansion of the GVB wavefunction are listed above the line in Table IV. At large R the GVB configurations are all important and are clearly dominant. For small R the HF configuration is the major configuration and some significant non-GVB configurations are found. In characterizing these configurations we use the notation described in footnote b of Table IV.

REFERENCES

1. Partially supported by a grant (GP-40783X) from the National Science Foundation.

2. R. S. Mulliken, Phys. Rev. 32, 880 (1928).

3. B. J. Moss, F. W. Bobrowicz, and W. A. Goddard III, J. Chem. Phys. to be submitted.

4. W. A. Goddard III, T. H. Dunning, Jr., W. J. Hunt, and P. J. Hay, Accts. Chem. Res. 6, 368 (1973).

5. T. H. Dunning, Jr., J. Chem. Phys. 53, 2823 (1970).

6. Written by F. W. Bobrowicz (Ph.D. Thesis, California Institute of Technology, 1974) and N. W. Winter, using the spin eigenfunction routines of R. C. Ladner (Ph.D. Thesis, California Institute of Technology, 1971). Modifications due to B. J. Moss, L. Harding, S. Walch and W. A. Goddard III.

7. P. Krupenie, J. Phys. Chem. Ref. Data 1, 423 (1972). This reference is more complete than those in Ref. 9.

8. G. Herzberg, Molecular Spectra and Molecular Structure. I. Spectra of Diatomic Molecules (Van Nostrand, New York, 1950).

9. B. Rosen, Spectroscopic Data Relative to Diatomic Molecules, (Pergamon Press, Oxford, 1970).

10. D. C. Cartwright, private communication.

11. Using the same basis set and a similar CI for the oxygen atom leads to excitation energies from $O(^3P)$ to $O(^1D)$ and $O(^1S)$ of 2.237 and 3.993 eV as compared to experimental values of 1.97 and 4.19 eV. This is one source of error in the calculations.

REFERENCES (continued)

12. (a) H. F. Schaefer III, J. Chem. Phys. 54, 2207 (1971);

(b) H. F. Schaefer III and W. H. Miller, J. Chem. Phys. 55, 4107

(1971); (c) P. E. Cade, unpublished, see Ref. 12a.

13. H. Taketa, H. Tatewaki, O. Nomura, and K. Ohno, Theoret.

Chim. Acta 11, 369 (1968).

14. K. Morokuma and H. Konishi, J. Chem. Phys. 55, 402 (1971).

15. We use mh to indicate 0.001 hartree. 1 mh = 0.002721 eV = 0.6275 kcal.

16. R. T. Pack, R. L. Snow, and W. T. Smith, J. Chem. Phys. 56, 926 (1972);

D. O. Ham, D. W. Trainor, and F. Kaufman, J. Chem. Phys. 53,

4395 (1970); R. E. Roberts, R. B. Bernstein, and C. F. Curtiss,

J. Chem. Phys. 50, 5163 (1969); S. W. Benson and T. Fueno,

J. Chem. Phys. 36, 1597 (1962).

17. P. Harteck and R. R. Reeves, Jr., Dis. Far. Soc. 37, 82 (1964).

18. V. Hasson and R. W. Nicholls, J. Phys. B4, 1789 (1971).

19. H. P. Broida and A. G. Gaydon, Proc. Roy. Soc. A222, 181 (1954);

V. Degen and R. W. Nicholls, J. Phys. B2, 1240 (1969).

20. V. Degen, Can. J. Phys. 46, 783 (1968); G. Herzberg, Can. J. Phys.

31, 657 (1953).

21. With zero overlap, $E_{^1\Delta_g} - E_{^3\Delta_u} = K_{x_\ell z_r} + \frac{1}{2}\left(K_{x_\ell x_r} + K_{z_\ell z_r} - [y_r x_\ell | x_r y_\ell]\right) = 0.1509$ mh at 6 a_0.

TABLE I. Configurations for the CI calculations (the $1\sigma_g$ and $1\sigma_u$ orbitals are doubly-occupied).

	$2\sigma_g$	$2\sigma_u$	$3\sigma_g$	$3\sigma_u$	$1\pi_{ux}$	$1\pi_{gx}$	$1\pi_{uy}$	$1\pi_{gy}$	Symmetry
(a)	2	2	2	0	2	1	2	1	g
	2	2	2	0	2	1	1	2	u
	2	2	2	0	1	2	2	1	u
	2	2	2	0	1	2	1	2	g
	2	2	1	1	2	1	2	1	u
	2	2	1	1	2	1	1	2	g
	2	2	1	1	1	2	2	1	g
	2	2	1	1	1	2	1	2	u
	2	2	0	2	2	1	2	1	g
	2	2	0	2	2	1	1	2	u
	2	2	0	2	1	2	2	1	u
	2	2	0	2	1	2	1	2	g
(b)	2	2	2	0	2	2	2	0	g
	2	2	2	0	2	2	1	1	u
	2	2	2	0	2	2	0	2	g
	2	2	2	0	2	0	2	2	g
	2	2	2	0	1	1	2	2	u
	2	2	2	0	0	2	2	2	g
	2	2	1	1	all six cases				
	2	2	0	2	all six cases				

TABLE II. Equilibrium parameters for various states of O_2.

| State | Excitation Energies | | | | | Equilibrium Properties | | | | | |
| | Adiabatic | | Vertical | | | D_e (eV) | | R_e (Å) | | ω_e (cm^{-1}) | |
	Calc	Expt[a]	Calculated R=1.2075	Calculated R=1.2375	Expt	Calc[b]	Expt[a]	Calc	Expt[a]	Calc	Expt[a]
$^1\Sigma_u^+$	10.187	(10.3)	13.599	12.961		0.920	(1.12)	1.655		652.8	
$^1\Delta_u$	8.794	(8.4)	12.023	11.406		0.556	(0.76)	1.648		627.2	
$2\ ^3\Sigma_g^-$	6.798		15.932	14.799		0.314		2.101		482.6	
$B\ ^3\Sigma_u^-$	6.308	6.174	9.422	8.812	~8.5[c]	0.805	1.007	1.625	1.604	667.8	709.1
$A\ ^3\Sigma_u^+$	4.249	4.389	6.507	5.981	~6.[d]	0.626	0.824	1.528	1.522	836.6	799.1
$C\ ^3\Delta_u$	4.173	4.307	6.375	5.848	~6.[d]	0.703	0.907	1.522	~1.5	858.9	~750.
$c\ ^1\Sigma_u^-$	3.937	4.099	6.115	5.594	~6.[d]	0.939	1.115	1.525	1.517	832.6	794.3
$b\ ^1\Sigma_g^+$	1.691	1.636	1.654	1.605	1.64	3.185	3.577	1.260	1.227	1505.1	1432.7
$a\ ^1\Delta_g$	1.089	0.982	1.014	0.989	0.98	3.787	4.232	1.249	1.216	1595.0	~1509.3
$X\ ^3\Sigma_g^-$	0	0	0	0	0	4.876	5.213	1.238	1.208	1692.7	1580.2

[a]Reference 7. For values in parentheses see text.
[b]Measured from the calculated separated-atom limit.
[c]Reference 10.
[d]Reference 18.

TABLE III. Calculated (GVB-CI) energies for the states of O_2 (subtract the quoted value from -149.0 to obtain the total energy).

	R = 2.0	2.285616	2.5	3.0	3.5	4.0	4.5	5.0	6.0
$X\,^3\Sigma_g^-$	0.71401	0.78030	0.77278	0.70471	0.64204	0.61167	0.60480	0.60362	0.60313
$a\,^1\Delta_g$	0.66951	0.73923	0.73559	0.67998	0.63387	0.61346	0.60665	0.60433	0.60313
$b\,^1\Sigma_g^+$	0.64210	0.71577	0.71562	0.66828	0.62888	0.61165	0.60588	0.60393	0.60298
$c\,^1\Sigma_u^-$	0.36996	0.55310	0.61054	0.63578	0.62261	0.61173	0.60667	0.60455	0.60325
$^3\Delta_u$	0.35857	0.54353	0.60173	0.62691	0.61317	0.60483	0.60318	0.60301	0.60295
$A\,^3\Sigma_u^+$	0.35171	0.53838	0.59761	0.62440	0.61153	0.60377	0.60256	0.60264	0.60280
$B\,^3\Sigma_u^-$	0.23510	0.43179	0.50188	0.54945	0.54120	0.52673	0.51942	0.51834	0.51979
$^1\Delta_u$	0.13894	0.33621	0.40739	0.45759	0.45245	0.44168	0.43664	0.43489	0.43364
$^1\Sigma_u^+$	0.07784	0.27836	0.35228	0.40610	0.40087	0.38719	0.37849	0.37440	0.37164
$2\,^3\Sigma_g^-$	-0.12144	0.19394	0.32905	0.47208	0.52105	0.53175	0.52621	0.52216	0.52025

TABLE IV. Energy contributions of dominant configurations of the GVB-CI wavefunction for the $X^3\Sigma_g^-$ state of O_2.

		Configuration				π_{ux}		π_{gx}		π_{uy}		π_{gy}		Energy Contribution (mh)			
No.	Character[b]	$2\sigma_g$	$2\sigma_u$	$3\sigma_g$	$3\sigma_u$	1	2	1	2	1	2	1	2	R_e[a]	$3a_0$	$4a_0$	$6a_0$
1	HF	2	2	2	0	2	0	1	0	2	0	1	0	2167.2	1295.4	312.7	98.0
2	C($3\sigma_g$)	2	2	0	2	2	0	1	0	2	0	1	0	12.4	25.2	89.3	94.9
3	I(π_{ux},π_{uy})	2	2	2	0	1	1	2	0	1	1	2	0	14.2	24.4	65.0	86.9
4	-	2	2	0	2	1	1	2	0	1	1	2	0	1.6	13.1	65.6	85.7
5	I($3\sigma_g$,π_u)	2	2	1	1	2	1	1	0	1	2	2	1	31.6	51.0	89.0	200.4
6	R(π_u,#1)	2	2	2	0	2	0	1	0	1	1	1	0	13.8	10.9	3.7	0.9
		2	2	2	0	1	1	1	0	2	0	1	0				
7	R(π_u,#2)	2	2	0	2	2	0	1	0	1	1	1	0	1.1	2.6	1.5	0.8
		2	2	0	2	1	1	1	0	2	0	1	0				
8	R(π_u,#5)	2	2	1	1	1	0	2	0	1	1	1	0	3.0	6.9	3.7	1.1
		2	2	1	1	1	1	1	0	1	0	2	0				
9	R(π_u,#5)	2	2	1	1	2	0	1	0	1	1	1	0	5.9	3.9	1.8	1.3
		2	2	1	1	1	1	1	1	2	0	1	1				
10	I($3\sigma_g$,π_g)	2	2	1	1	2	1	0	0	2	0	1	0	7.2	6.0	2.5	1.1
		2	2	1	1	2	0	1	0	2	1	0	0				
11	I(π_u,π_g)	2	2	2	0	2	0	2	0	2	0	0	0	3.6	1.8	0.0	0.2
		2	2	2	0	2	1	0	0	1	0	2	0				
12	C(π_u)	2	2	2	0	0	0	2	1	2	0	1	0	2.4	1.9	0.8	0.3
		2	2	2	0	2	0	1	0	0	0	2	1				
13	R($2\sigma_u$,#1)	2	1	2	1	2	0	1	0	2	0	1	0	1.7	1.1	0.3	0.0
14	C($2\sigma_u$)	2	0	2	2	2	0	1	0	2	0	1	0	1.1	2.3	0.7	0.0

[a] $R = 2.285616\ a_0$.

[b] R indicates an orbital readjustment effect (single excitation); C indicates correlation of a particular doubly-occupied orbital; I indicates an interpair correlation effect.

TABLE V. Energy contributions of dominant configurations of the GVB-CI wavefunctions for the $^1\Delta_g^+$ and $^1\Sigma_g^+$ states of O_2.

No.	Character	$2\sigma_g$	$2\sigma_u$	$3\sigma_g$	$3\sigma_u$	π_{ux} 1	π_{ux} 2	π_{gx} 1	π_{gx} 2	π_{uy} 1	π_{uy} 2	π_{gy} 1	π_{gy} 2	$^1\Delta_g^+$ (mh)	$^1\Sigma_g^+$ (mh)
1	HF	2	2	2	0	2/2		0/2		2/2		2/0		303.6	253.3
2	$C(\pi_u)$	2	2	2	0	0/2		2/2		2/0		2/2		30.8	42.9
3	$C(3\sigma_g)$	2	2	0	2	2/2		0/2		2/2		2/0		14.6	14.1
4	-	2	2	0	2	0/2		2/2		2/0		2/2		2.5	3.1
5	$I(3\sigma_g,\pi_u)$	2	2	1	1	1/2		1/2		2/1		2/1		29.7	26.9
6	$I(\pi_g,\pi_u)$	2	2	2	0	1/2	0/1	1/1	0/0	2/1	1/0	1/1	0/0	10.3	4.4
7	$I(3\sigma_g,\pi_g)$	2	2	1	1	2/2	0/1	0/1	0/0	2/2	1/0	0/0	0/0	8.5	9.1
8	$I(\pi_{ux},\pi_{uy})$	2	2	2	0	1/1	0/0	1/2	0/1	1/1	0/0	2/1	1/0	2.2	2.4
9	$I(3\sigma_g,\pi_u)$	2	2	1	1	2/1	0/0	0/2	0/1	1/2	0/0	2/0	1/0	3.4	3.5
10	$I(3\sigma_g,\pi_g,\#2)$	2	2	1	1	0/2	0/1	2/1	0/0	2/0	1/0	1/2	0/0	2.3	2.2
11	$R(\pi_u,\#5)$	2	2	1	1	2/1	0/0	2/0	0/1	1/2	0/0	0/2	1/0	3.4	3.5
12	$C(\pi_g)$	2	2	2	2	2	0	0	0	2	0	0	0	0.0	1.3
13	$C(2\sigma_g)$	0	2	2	0	2	0	2	0	2	0	2	0	0.0	1.9
14	$C(2\sigma_u)$	2	0	2	0	2	0	2	0	2	0	2	0	0.0	6.4

TABLE VI. Energy contribution of dominant configurations of the GVB-CI wavefunction for the $^1\Sigma_u^-$, $^3\Delta_u^-$, $^3\Sigma_u^-$, and $^1\Delta_u^-$ state of O_2.

No.	Character	Configuration																Energy Contribution (mh)			
		$2\sigma_g$	$2\sigma_u$	$3\sigma_g$	$3\sigma_u$	π_{ux} 1	2	π_{gx} 1	2	π_{uy} 1	2	π_{gy} 1	2				$^1\Sigma_u^-$	$^3\Delta_u^-$	$^3\Sigma_u^-$	$^1\Delta_u^-$
1	HF	2	2	2	0	1 2		2 1		2 1		1 2					506.8	422.2	166.2	81.7
2	C($3\sigma_g$)	2	2	0	2	1 2		2 1		2 1		1 2					21.5	20.8	46.6	3.9
3	I($3\sigma_g,\pi_g$)	2	2	1	1	2		1		2		1					3.7	1.4	66.5	67.1
4	I($3\sigma_g,\pi_u$)	2	2	1	1	1		2		1		2					1.3	5.6	34.1	31.8
5	R(π_u)	2	2	2	0	1 1	0 1	2 1	0 0	1 1	1 0	1 2	0 0				2.8	2.0	21.4	19.5
6	R(π_g)	2	2	2	0	1 2	0 0	1 1	1 0	2 1	0 0	1 2	0 1				0.6	1.6	9.4	8.2
7	R($2\sigma_u$)	2	1	2	1	1 2	0 0	2 1	0	2 1	0 0	1 2	0 0				0.6	2.1	4.1	3.1
8	I($3\sigma_g,\pi_g$)	2	2	1	1	1 2	1 0	1 1	0 0	2 1	0 1	1 1	0 0				13.8	15.0	3.1	2.9
9	I($3\sigma_g,\pi_g$)	2	2	1	1	1 2	0 1	2 0	0 0	2 1	1 0	1 2	0 0				7.5	7.0	0.6	0.5
10	I($3\sigma_g,\pi_u$)	2	2	1	1	1 1	1 0	2 1	0 1	1 1	1 0	1 2	1 0				5.9	5.8	0.5	0.6
11	I($3\sigma_g,\pi_u$)	2	2	1	1	0 2	0 0	2 1	0 0	2 0	0 0	1 2	0 1				2.8	2.7	0.4	0.3
12	I(π_{gx},π_{gy})	2	2	2	0	2 2	0 1	1 0	0 0	2 2	1 0	0 1	0 0				2.9	0.6	22.3	15.6
13	I(π_{ux},π_{uy})	2	2	2	0	0 1	0 0	2 2	0 1	1 0	0 0	2 2	0 1				0.6	0.1	3.5	2.7
14	–	2	2	0	2	2 2	1 0	0 1	0 0	2 2	0 1	1 0	0 0				0.1	0.0	3.1	2.9
15	–	2	2	0	2	1 1	0 1	2 1	0 0	1 1	1 0	1 2	0 0				0.1	0.1	2.0	2.0
16	R($2\sigma_g$, #3)	1	2	2	1	2		1	1 0	2		1					0.8	0.2	7.3	7.7
17	R($2\sigma_g$, #4)	1	2	2	1	1		2	0	1		2					0.4	0.1	1.3	1.0

TABLE VII. Energy contribution of dominant configurations of the GVB-CI wavefunction for the $^3\Delta_u^+$, $^3\Sigma_u^+$, $^1\Delta_u^+$ and $^1\Sigma_u^+$ state of O_2.

No.	Character	2σg	2σu	3σg	3σu	πux 1	πux 2	πgx 1	πgx 2	πuy 1	πuy 2	πgy 1	πgy 2	$^3\Delta_u^+$	$^3\Sigma_u^+$	$^1\Delta_u^+$	$^1\Sigma_u^+$
1	HF	2	2	2	0	1	2	1	2	2	1	2	1	133.7	124.0	443.8	345.1
2	C(3σg)	2	2	0	2	1	2	1	2	2	1	2	1	19.5	19.5	4.4	3.8
3	I(3σg,πg)	2	2	1	1	2	2	0	2	2	2	2	0	1.4	1.4	66.5	68.8
4	I(3σg,πu)	2	2	1	1	0	2	2	2	2	0	2	2	0.6	0.6	31.9	29.0
5	R(πg)	2	2	2	0	1	2	0	2	2	1	2	0			3.9	3.5
6	R(πu)	2	2	2	0	0	2	1	2	2	0	2	1			10.5	9.3
7	R(2σu)	2	1	2	1	1	2	1	2	2	1	2	1	2.0	2.0	3.7	4.6
8	I(3σg,πg)	2	2	1	1	1	2	1	1	2	1	1	1	13.3	13.2		
9	I(3σg,πg)	2	2	1	1	1	2	0	2	2	1	2	0	6.3	6.3		
10	I(3σg,πu)	2	2	1	1	1	1	1	2	1	1	2	1	5.6	5.7		
11	I(3σg,πu)	2	2	1	1	0	2	1	2	2	0	2	1	2.5	2.5		
12	I(πgx,πgy)	2	2	2	0	2	2	0	1	2	2	0	1			17.9	10.9
13	I(πux,πuy)	2	2	2	0	0	1	2	2	0	1	2	2			2.8	2.2
14	-	2	2	0	2	2	2	0	1	2	2	1	0			3.0	2.7
15	I(πu,πg)	2	2	2	0	2	1	0	2	2	1	2	0			4.0	2.3
16	I(πu,πg)	2	2	2	0	0	2	2	1	2	0	1	2			8.3	7.6
17	R(2σg,#3)	1	2	2	1	2	2	0	2	2	2	2	0			7.8	8.3
18	C(2s)	{1,2,0}	{1,0,2}	{2,1,1}	{0,1,1}	2	2	2	2	2	2	2	2			0.0 / 0.0 / 0.0	30.5 / 3.0 / 2.2

Energy Contribution (mh)